Transport Properties of Isobutane

Johan C. Nieuwoudt

Institute for Physical Science and Technology, University of Maryland, College Park, Maryland 20742

Bernard Le Neindre and Roland Tufeu

Laboratoire des Interactions Moléculaires et des Hautes Pressions, CNRS, Centre Universitaire Paris-Nord, 93430 Villetaneuse, France

Jan V. Sengers*

Institute for Physical Science and Technology, University of Maryland, College Park, Maryland 20742, and Thermophysics Division, National Bureau of Standards, Gaithersburg, Maryland 20899

Representative equations are presented for the viscosity and thermal conductivity of isobutane as a function of temperature and density. The equations are based on existing experimental data for the viscosity and new experimental data for the thermal conductivity of isobutane.

Introduction

There exists considerable interest in reliable information for the thermophysical properties of isobutane. The interest is generated in part by the possible use of isobutane as a working fluid in binary geothermal power cycles. For this reason scientists at the National Bureau of Standards have recently developed new representative equations for the thermodynamic properties of isobutane (*1-5*). The purpose of the present paper is to supplement this information with representative equations for the viscosity and thermal conductivity of isobutane.

A survey of the literature revealed an adequate amount of existing experimental data to develop a representative equation for the viscosity of isobutane (*6-8*). However, experimental information on the thermal conductivity of isobutane appeared to be extremely limited (*6*, *9*) and it became necessary to conduct an experimental investigation of the thermal conductivity of isobutane. The new experimental data obtained for the thermal conductivity of isobutane are included in this paper.

Equations of State

The transport properties are usually measured as a function of temperature and pressure. To convert the experimental temperatures T and pressures P into densities ρ we need a reliable equation of state. Furthermore, the proposed representative equation for the thermal conductivity contains in the critical region the compressibility and thermal pressure coefficient which are derivatives of the equation of state. For the results presented in this paper, we have adopted the equations of state previously published in this journal (*2*, *3*). In a region around the critical point specified by

$$405\ \text{K} \leq T \leq 438\ \text{K} \qquad (1)$$

$$150\ \text{kg m}^{-3} \leq \rho \leq 290\ \text{kg m}^{-3}$$

we use the scaled equation of state of Levelt Sengers, Kamgar-Parsi, and Sengers (*3*). Outside this critical region we use the global equation of state of Waxman and Gallagher (*2*). The latter equation of state is valid at temperatures from 250 to 600 K and pressures up to 40 MPa. An alternative global equation of state valid at temperatures from 114 to 700 K and pressures up to 70 MPa has been presented by Goodwin and Haynes (*5*). The relationship between the two global equations of state has been discussed by Waxman and Gallagher (*2*).

We prefer to formulate representative equations for the transport properties that have dimensionless coefficients. For this purpose we introduce the following dimensionless quantities

$$\bar{T} = T/T_c, \quad \bar{\rho} = \rho/\rho_c, \quad \bar{P} = P/P_c \qquad (2a)$$

$$\bar{\eta} = \eta/\eta_r, \quad \bar{\lambda} = \lambda/\lambda_r \qquad (2b)$$

with

$$T_c = 407.84\ \text{K}, \quad \rho_c = 225.5\ \text{kg m}^{-3}, \quad P_c = 3.629 \times 10^6\ \text{Pa} \qquad (3a)$$

$$\eta_r = 1 \times 10^{-6}\ \text{Pa s}, \quad \lambda_r = 1 \times 10^{-3}\ \text{W m}^{-1}\ \text{K}^{-1} \qquad (3b)$$

The reference values adopted for the temperature, density, and pressure as defined by eq 3a are equal to the values most recently reported for the critical parameters of isobutane (*3*).

Experimental Thermal Conductivity Data

The thermal conductivity was measured with a concentric-cylinder apparatus. The experimental procedure was identical with that used previously in measuring the thermal conductivity of *n*-butane (*10*). The fluid is located in the annular gap between two coaxial cylinders with the axis in the vertical direction. The thermal conductivity was determined by measuring the temperature difference between the inner and outer cylinder as a function of the energy dissipated from the inner cylinder. The temperature differences between the two cylinders varied from about 0.1 °C close to the critical point to about 2 °C far away from the critical point; this temperature difference was measured with an accuracy of approximately ±0.003 °C. The measurements were performed at temperatures from room temperature to 350 °C and at pressures up to 100 MPa. The temperature was measured with an accuracy of ±0.02 °C and the pressure with an accuracy of 0.1%.

To determine the coefficient of thermal conductivity we need to consider corrections due to heat transferred by radiation, corrections due to parasitic heat flow from the inner to the outer cylinder through the solid boundaries, the effects of a possible temperature jump at the boundaries of the fluid layer and surfaces of the cylinders, and the possible presence of convection (*11*). We calculated the radiation correction from Stefan-Boltzmann's radiation law assuming that the absorption of radiation by the fluid could be neglected. The correction for parasitic heat losses through the solid parts of the cell was determined from a set of calibration measurements with argon and neon for which the thermal conductivity is known with

0021-9568/87/1732-0001$01.50/0

considerable accuracy (*12–14*). These calibration measurements were performed as a function of temperature and at pressures of about 5 MPa. The effect of any temperature jump is potentially significant at low pressures and is inversely proportional to the thickness of the fluid layer. While most of our experimental data were obtained with a gap width of 0.2 mm between the cylinders, we also made some measurements at lower pressures with a larger gap width of 0.4 mm. The thermal conductivity λ of the fluid is related to the heat flow Q transmitted radially from the inner cylinder by

$$Q = K^{-1}\lambda\Delta T \tag{4}$$

where ΔT is the temperature difference between the cylinders and K the cell constant (*10*). Convection is likely to occur in the vicinity of the critical point. Assuming the convective flow to be laminar, we estimated the associated heat flow Q_c from the relation

$$Q_c = N_{Ra}\frac{2\pi r}{720}\lambda\Delta T \tag{5}$$

where N_{Ra} is the Rayleigh number and r the mean radius of the annual fluid layer. In selecting the experimental pressures and temperatures near the critical point we made sure that the correction Q_c/Q never exceeded 3%.

The thermal conductivity was determined with a reproducibility of 1% and an estimated accuracy of about 2% except in the critical region where the measurements become very sensitive to small errors in pressure and temperature. The isobutane was obtained commercially and the purity as estimated by the supplier was 99.95 mol %.

The experimental data, obtained with the gap width d equal to 0.2 mm, are presented in Table I. The data were taken at temperatures from room temperature to about 360 °C and at pressures up to 100 MPa and cover the gaseous region, the supercritical region, and the liquid region. The thermal conductivity was obtained as a function of temperature and pressure and the densities were calculated from the equations of state mentioned in the preceding section. In principle, the validity of the equation of state of Waxman and Gallagher is restricted to pressures up to 40 MPa (*2*). At pressures above 40 MPa we, therefore, also calculated the densities from the equation of state of Goodwin and Haynes which covers a larger pressure range (*5*). It was found that the densities thus obtained agreed with the densities calculated from the extrapolated equation of Waxman and Gallagher within 0.5%.

In addition we obtained some thermal conductivity data at low pressures with a gap width d equal to 0.4 mm; these data are presented in Table II. The thermal conductivity λ_0 of gaseous isobutane in the low density limit is shown in Figure 1a as a function of temperature. For this purpose we plotted the data, obtained with d = 0.2 mm and listed in Table I, as a function of density and determined the values in the limit $\rho \rightarrow 0$. In addition, values were obtained from the data, taken at low pressures with d = 0.4 mm and listed in Table II, with a minor correction for the difference between zero pressure and the actual experimental pressures. From the fact that the two sets of λ_0 values agree well within the experimental accuracy we conclude that the effects of any temperature jumps at the fluid boundaries are negligibly small even at the lowest pressures.

Experimental values for the thermal conductivity of gaseous isobutane have been reported by Mann and Dickens (*15*), Lambert et al. (*16*), Kazaryan and Ryabstev (*9*), and Parkinson and Gray (*17*). The values of λ_0 found in the literature are also included in Figure 1a. Our data are in satisfactory agreement with the data of Kazaryan and Ryabstev (*9*) and the value reported by Lambert et al. (*1b*). We reject the value quoted by Mann and Dickens (*15*) as unreliable, while the values obtained by Parkinson and Gray (*17*) appear somewhat high as compared to all other data.

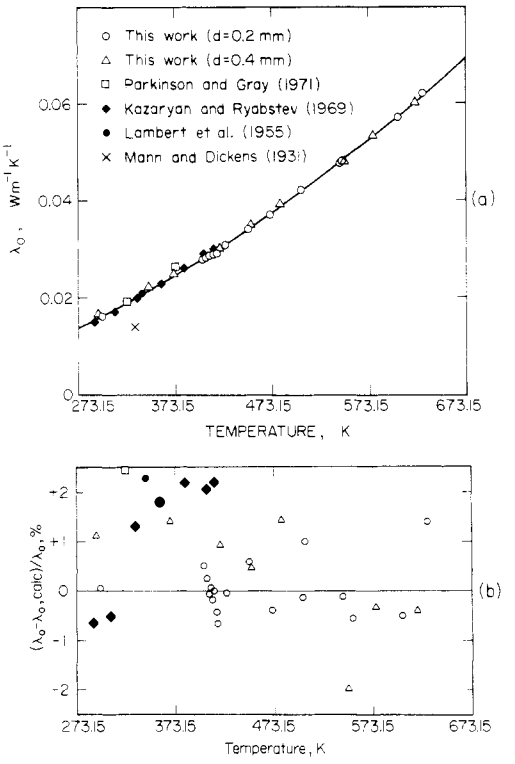

Figure 1. Comparison between the experimental data for the thermal conductivity λ_0 of the dilute gas and the values calculated from eq 13.

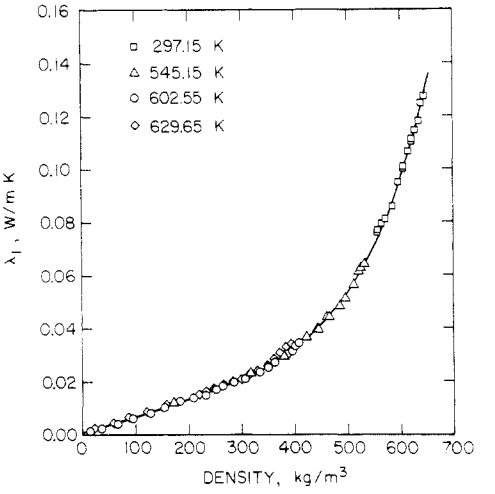

Figure 2. Excess thermal conductivity λ_1 deduced from our experimental data as a function of density at temperatures well above and below the critical temperature. The solid curve represents the values calculated from eq 14.

To describe the behavior of the thermal conductivity as a function of density it is convenient to introduce an excess thermal conductivity as the difference between the thermal conductivity $\lambda(T,\rho)$ at the actual density ρ and the thermal conductivity $\lambda_0(T) = \lambda(T,0)$ at zero density at the same temperature

$$\lambda_1 \equiv \lambda(T,\rho) - \lambda_0(T) \tag{6}$$

In Figure 2 we have plotted the excess thermal conductivity λ_1 deduced from our experimental data as a function of density at temperatures well below and above the critical temperature. With the exception of a few data points, the excess thermal conductivity λ_1 is to a good approximation independent of the temperature and a function only of the density. This phenom-

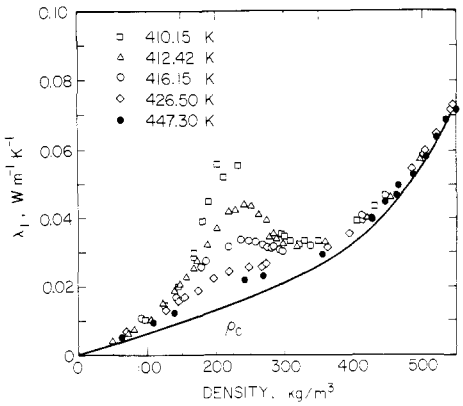

Figure 3. Excess thermal conductivity λ_1 deduced from our experimental data as a function of density at temperatures in the vicinity of the critical temperature. The solid curve represents the values calculated from eq 14.

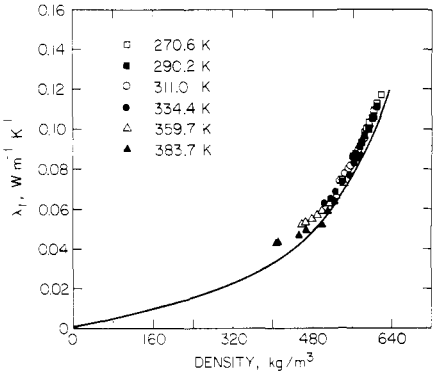

Figure 4. Excess thermal conductivity λ_1 deduced from the data of Kazaryan and Ryabstev (*9*) as a function of density. The solid curve represents the values calculated from eq 14.

enon is similar to that observed for many other fluids in corresponding ranges of temperatures and densities (*18*). The excess thermal conductivity λ_1 deduced from our experimental data at temperatures closer to the critical temperature is shown in Figure 3. Here we observe an enhancement of the thermal conductivity in a wide range around the critical point which depends strongly on both ρ and T. Again this phenomenon is similar to the behavior of the thermal conductivity observed for other fluids in the critical region (*18*).

To our knowledge the thermal conductivity of isobutane at elevated pressures has only been measured previously by Kazaryan and Ryabstev (*9*). In Figure 4 we show the excess thermal conductivity λ_1 deduced from the data reported by Kazaryan and Ryabstev at temperatures between 271 and 384 K. A comparison with our experimental data reveals the existence of sizable systematic differences of about 10%. Kazaryan and Ryabstev (*9*) obtained also a few data points in the critical region which indicate the existence of the critical enhancement in the thermal conductivity but which are too sparse to make a quantitative estimate of the effect.

Representative Equation for Viscosity

The available literature on viscosity measurements for isobutane is summarized in Table III. After reviewing the literature we concluded that the measurements of Abe et al. (*23*) yield the most accurate information for the viscosity in the dilute gas state, while the measurements of Agayev and Yusibova (*7*) and those of Diller and Van Poolen (*8*) yield the most comprehensive information for the viscosity in the compressed gas and liquid states. Accordingly, we have developed our representative equation for the viscosity on the basis of these three data sets.

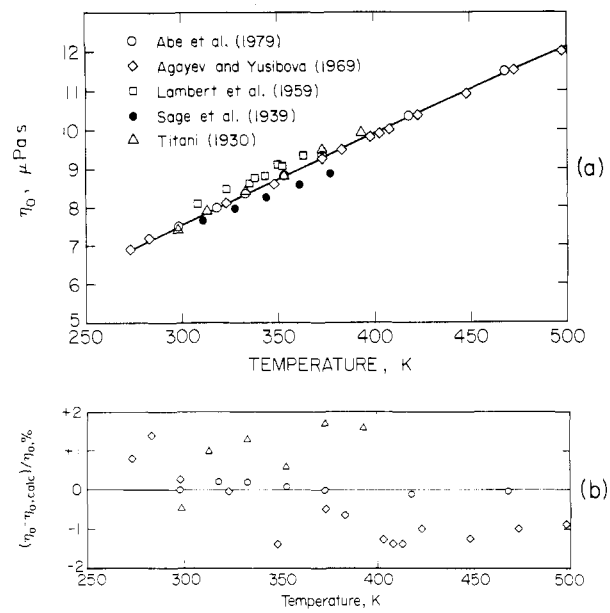

Figure 5. Comparison between the experimental data for the viscosity η_0 of the dilute gas and the values calculated from eq 8.

Our proposed representative equation for the viscosity of isobutane has the form

$$\bar{\eta} = \bar{\eta}_0(\bar{T}) + \frac{\bar{\eta}_1(\bar{\rho})}{1 + e^{-z(\bar{T}-\bar{T}_0)}} + \frac{\bar{\eta}_2(\bar{T},\bar{\rho})}{1 + e^{z(\bar{T}-\bar{T}_0)}} \tag{7}$$

with

$$\bar{\eta}_0(\bar{T}) = \frac{\bar{T}^{1/2}}{H_{00} + H_{01}/\bar{T}} \tag{8}$$

$$\bar{\eta}_1(\bar{\rho}^l) = \sum_{i=1}^{7} H_{1i}\,\bar{\rho}^i \tag{9}$$

$$\bar{\eta}_2(\bar{T},\bar{\rho}) = H_{20}\exp\left(\frac{H_{21}}{\bar{T}} + \frac{H_{22}}{\bar{T}^3}\right)\frac{\bar{\rho}}{1 - \bar{\rho}(H_{23} + H_{24}\bar{T})} \tag{10}$$

The values of the coefficients H_{ij} and z and of the reduced temperature $\bar{T}_0$ are presented in Table IV. The number of terms in these equations and the values of the parameters were determined with the aid of an optimization procedure proposed by Wagner (*24–26*).

The term $\bar{\eta}_0(\bar{T})$ represents the viscosity of the dilute gas as a function of temperature. The functional form chosen for $\bar{\eta}_0(\bar{T})$ as a function of is $\bar{T}$ similar to the one used for the viscosity of water vapor and steam at low pressures (*27*,*28*). The available viscosity data for the dilute gas are shown in Figure 5a. We judge that the data of Abe et al. have the highest accuracy and they were used to determine the coefficients H_{00} and H_{01} in eq 8 for $\bar{\eta}_0(\bar{T})$. The data of Sage and co-workers (*20*) and those of Lambert and co-workers (*16*) are in substantial disagreement with the more accurate data of Abe et al. In Figure 5b we show the differences between the experimental data of Abe et al. (*23*), of Agayev and Yusibova (*7*), and of Titani (*19*) and the values calculated from our equation. The equation reproduces the data of Abe et al. within a maximum deviation of 0.4% and with an average deviation of 0.2%. It also agrees with the data of Agayev and Yusibova and those of Titani within the estimated error of these data.

The function $\bar{\eta}_1(\bar{\rho})$ represents the excess viscosity $\eta_1 = \eta - \eta_0$ at temperatures above 0 °C. In Figure 6 we show the excess viscosity η_1 deduced from the data of Agayev and Yusibova (*7*). In the temperature range of these data the excess viscosity η_1 can be approximated by a function of density only.

Table I. Experimental Thermal Conductivity Data[a]

T, °C	P, MPa	ρ, kg m^{-3}	$10^3\lambda$, W m^{-1} K^{-1}	T, °C	P, MPa	ρ, kg m^{-3}	$10^3\lambda$, W m^{-1} K^{-1}
25.17	2.38	555	93.1	142.71	9.98	413	70.0
24.51	2.18	555	93.7	142.58	15.86	447	76.0
24.43	6.30	563	96.3				
24.27	10.60	571	97.9	145.39	2.78	66.0	35.6
24.54	19.80	584	102.7	144.80	3.81	127	43.0
24.37	30.50	596	111.9	144.52	4.12	183	53.8
23.71	40.60	606	117.4	144.52	4.19	206	58.1
24.62	40.10	605	118.1	144.58	4.24	224	60.1
24.35	51.40	615	123.8	144.68	4.29	239	60.6
24.11	60.00	621	127.8	144.77	4.35	254	60.2
23.88	70.00	628	131.9	144.88	4.43	269	59.6
23.32	80.20	634	135.4	145.05	4.57	289	58.9
23.13	90.00	641	142.3	145.15	4.68	299	58.9
23.04	100.00	646	145.0	145.30	4.85	311	58.9
				145.51	5.08	323	59.4
136.70	3.24	96.6	38.9	146.59	10.17	407	67.5
138.44	3.55	120	42.2	146.85	14.46	435	71.8
138.16	3.66	137	46.3				
137.93	3.73	155	51.4	153.77	3.00	69.9	37.8
137.12	3.72	165	57.1	153.22	4.07	127	44.1
137.36	3.75	175	64.7	153.19	4.27	146	46.9
137.00	3.74	180	67.7	153.81	4.35	153	47.5
137.27	3.76	185	73.7	153.00	4.50	177	50.2
137.02	3.76	210	79.7	152.99	4.63	200	53.8
137.08	3.78	223	84.3	152.97	4.76	223	55.7
137.29	3.88	291	64.3	152.96	4.94	252	56.9
137.25	3.91	296	63.6	153.01	5.10	271	57.0
137.26	3.96	304	62.3	153.06	5.15	275	57.6
137.24	4.07	317	60.9	153.91	7.50	360	62.3
137.18	4.18	326	62.1	153.58	10.00	393	66.3
137.19	4.60	347	62.1	153.59	20.70	454	76.9
137.23	7.83	404	67.8	152.94	31.60	486	85.5
137.00	11.07	430	72.1	154.23	39.60	502	89.3
				153.25	40.50	505	90.7
139.36	2.23	49.8	33.1	153.60	50.00	521	95.4
139.11	2.84	72.0	35.3	153.57	65.30	542	102.3
138.72	3.01	80.8	36.5	153.56	67.50	545	103.5
138.52	3.42	107	39.5				
140.02	3.60	121	43.6	175.65	3.07	63.3	39.1
139.89	3.72	136	47.0	175.32	4.37	109	43.4
139.73	3.75	144	48.7	175.15	4.98	141	46.4
139.71	3.79	153	50.6	175.26	6.50	246	56.1
139.70	3.82	161	52.1	175.17	7.00	273	57.2
139.69	3.84	165	53.8	176.15	10.50	354	63.3
139.52	3.87	180	58.4	177.34	20.10	424	73.8
139.49	3.88	192	62.8	176.22	20.50	427	73.6
139.43	3.91	210	69.0	177.52	25.20	445	78.5
139.27	3.91	228	71.2	176.26	30.50	463	80.6
139.26	3.93	241	72.8	177.66	31.50	464	83.3
139.38	3.94	246	73.0	176.15	40.60	487	86.7
139.39	3.97	258	70.5	176.09	50.30	506	92.0
139.40	4.00	270	68.7	176.45	60.50	521	97.3
139.42	4.03	280	64.7	175.99	70.70	535	102.4
139.16	4.05	291	63.2	176.10	82.50	549	105.4
138.49	4.01	294	62.7	176.03	90.00	557	110.1
138.53	4.10	307	61.3				
138.53	4.29	323	60.8	198.65	1.37	22.1	39.6
138.65	5.24	361	62.2	198.44	2.70	48.2	41.1
139.40	10.10	419	69.2	198.18	4.68	101	45.4
139.49	16.40	453	75.1	197.86	6.10	157	50.4
139.13	31.10	497	86.4	198.03	7.51	220	55.6
				198.59	8.91	269	59.5
143.84	3.30	90.9	40.1	198.87	10.23	301	61.3
143.81	3.87	138	45.5	198.88	11.62	325	63.2
143.50	4.03	172	53.4	199.03	13.30	347	65.0
143.48	4.05	177	54.9	199.20	14.65	360	66.6
143.47	4.13	206	58.9	199.27	15.90	371	68.0
143.44	4.17	224	62.1	199.54	17.30	381	69.8
143.44	4.20	236	62.4	198.74	18.70	391	71.2
143.44	4.23	247	62.4	198.65	20.20	400	72.0
143.46	4.27	259	61.6	198.67	21.90	409	73.3
143.46	4.30	266	61.0	198.44	24.50	421	74.9
143.48	4.33	272	60.7	197.73	27.30	433	76.8
143.25	4.35	280	61.0	197.56	28.90	439	77.7
143.48	4.41	286	60.1	197.47	30.10	443	79.7
143.53	4.49	296	59.7	196.49	33.50	454	82.1
142.79	5.08	338	61.4				
143.91	10.05	411	68.6	230.79	4.07	70.6	47.1
				231.56	20.30	363	71.3

Table I (Continued)

T, °C	P, MPa	ρ, kg m^{-3}	$10^3\lambda$, W m^{-1} K^{-1}	T, °C	P, MPa	ρ, kg m^{-3}	$10^3\lambda$, W m^{-1} K^{-1}
229.83	30.00	414	78.1	272.48	42.00	421	85.1
232.00	40.40	445	84.2	272.67	50.00	442	88.2
231.77	50.40	469	88.7	271.75	51.00	445	89.9
231.46	60.50	488	94.0	272.72	58.80	462	92.5
230.96	70.00	504	97.7	272.90	59.80	463	92.5
231.06	69.50	503	98.8	272.75	71.30	484	96.8
230.44	78.80	516	103.3	272.58	78.30	495	99.5
230.29	87.30	527	106.9	272.15	89.50	511	105.0
230.09	100.20	542	112.0	271.95	99.00	522	110.2
				271.86	101.00	525	111.2
232.59	1.16	16.9	44.6	271.84	106.50	531	112.9
232.44	2.74	43.5	46.0				
232.18	4.63	82.7	48.5	330.60	1.08	12.8	58.3
231.95	6.30	125	51.8	330.52	2.83	35.0	59.6
231.95	8.15	179	55.9	330.39	4.98	64.6	61.2
231.81	8.41	187	58.8	330.28	6.93	93.4	63.4
231.92	10.80	248	61.1	330.19	9.09	126	65.3
232.06	12.15	275	63.1	329.95	10.20	144	67.5
232.02	13.45	296	64.6	329.90	12.90	183	69.9
232.00	14.80	314	66.4	329.82	14.80	209	71.2
232.05	16.30	330	67.7	329.86	16.70	231	72.2
232.54	17.70	342	68.9	329.92	18.50	251	74.5
232.43	18.80	351	69.8	329.88	19.90	264	75.9
232.77	20.10	361	70.4	329.94	22.30	285	77.1
232.91	21.10	367	71.5	329.87	25.20	306	78.7
233.01	23.00	378	72.9	329.88	27.70	321	80.3
233.11	24.40	386	73.9	329.88	29.80	333	81.2
233.20	25.90	393	75.2	328.84	33.10	350	82.8
233.18	26.85	398	76.3	329.76	35.90	362	84.9
233.06	28.50	405	77.6	329.70	39.20	375	86.7
232.97	30.40	413	78.9	329.74	42.10	385	88.0
				329.82	45.20	395	89.2
269.90	2.50	35.3	50.6	329.92	46.80	400	91.1
269.47	4.18	63.2	52.4	330.04	49.10	406	91.0
269.21	5.90	95.6	54.9				
269.00	7.38	126	57.0	357.62	1.09	22.9	63.0
268.95	9.50	172	60.6	357.48	4.78	57.8	65.1
268.79	11.00	203	62.7	357.18	6.89	86.0	67.2
268.91	12.60	232	63.7	357.12	9.50	122	69.1
269.37	13.80	251	65.4	357.14	12.20	158	72.1
269.35	15.00	268	66.6	357.46	16.20	207	75.6
269.67	16.55	286	68.6	357.45	17.40	220	76.1
269.71	18.20	304	70.0	357.41	18.80	234	77.2
269.64	19.75	318	71.1	357.41	20.30	248	78.2
269.65	21.05	328	72.2	357.34	22.40	265	79.5
269.64	22.55	339	72.6	357.39	24.80	283	80.9
269.59	24.25	350	74.9	357.46	27.20	299	82.1
267.17	27.90	372	76.1	357.38	29.80	315	83.5
267.11	29.80	381	78.0	357.29	32.80	330	84.9
266.78	33.30	396	79.2	357.22	36.70	348	87.3
				357.31	40.00	361	88.7
272.35	9.60	171	60.4	357.31	42.90	372	90.8
272.36	19.90	316	71.4	356.92	46.90	385	93.0
272.76	30.20	379	85.1	356.92	49.80	394	94.4

[a] Obtained with a gap width d = 0.2 mm.

Table II. Experimental Thermal Conductivity Data[a]

T, °C	P, MPa	$10^3\lambda$, W m^{-1} K^{-1}
20.3	0.26	16.9
72.3	0.28	22.6
97.2	0.13	24.3
97.3	0.24	24.9
146.0	0.11	30.4
146.0	0.14	30.6
178.2	0.13	34.7
208.5	0.12	39.5
273.8	0.12	47.7
304.4	0.26	53.6
348.3	0.28	60.5

[a] Obtained with a gap width d = 0.4 mm.

Table III. Data Reported for the Viscosity of Isobutane (*6*)

first author	year	region[a]	ref
Titani	1930	1	*19*
Sage	1939	2	*20*
Lipkin	1942	3	*21*
Lambert	1955	1	*16*
Gonzalez	1966	2	*22*
Agayev	1969	2	*7*
Abe	1979	1	*23*
Diller	1985	3, 4	*8*

[a] Regions: 1, gas at atmospheric pressure; 2, compressed gas and liquid; 3, liquid at saturation; 4, compressed liquid.

The viscosity of the liquid measured by Diller and Van Poolen (*8*) at lower temperatures is shown in Figure 7. At these lower temperatures the excess viscosity η_1 does depend on temperature. Therefore at lower temperatures we represent the behavior of the excess viscosity by the function $\bar{\eta}_2(\bar{T},\bar{\rho})$ which is a slight generalization of the free-volume equation proposed by Diller and Van Poolen (*8*). The functions $1 + \exp[\pm z(\bar{T} - \bar{T}_0)]$ in eq 7 are switching functions to account for the crossover from the lower temperature to the higher temperature behavior of the excess viscosity.

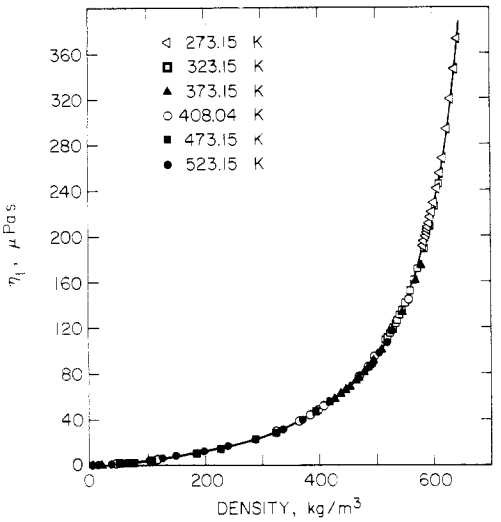

Figure 6. Excess viscosity η_1 deduced from the data of Agayev and Yusibova (*7*) as a function of density. The solid curve represents the values calculated from eq 9.

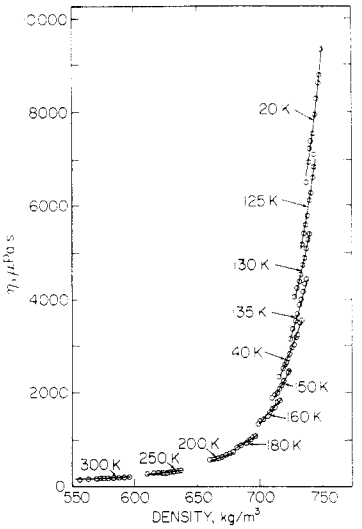

Figure 7. Viscosity data of Diller and Van Poolen (*8*) as a function of density. The solid curves represent the values calculated from eq 7.

The viscosity of gases is known to exhibit a singular behavior at the critical point. However, unlike the critical behavior observed for the thermal conductivity, the critical enhancement of the viscosity is weak and restricted to temperatures very close to the critical temperature (*29*, *30*). In the absence of any experimental information on the critical enhancement in the viscosity of isobutane we have neglected the effect.

A comparison between the experimental data of Agayev and Yusibova (*7*), of Diller and Van Poolen (*8*), and of Gonzalez and Lee (*22*) is presented in Figure 8. Our equation reproduces the experimental data with a standard deviation of about 3%. The old data of Sage et al. (*20*) appear to be inconsistent with the other available experimental information and are not further considered here. The older data of Lipkin et al. (*21*) for the saturated liquid have been superseded by the new data of Diller and Van Poolen (*8*).

We estimate that eq 7 represents the viscosity of isobutane with an accuracy of about ±3% in a range of temperatures and densities approximately bounded by

$$120\ \text{K} \leq T \leq 550\ \text{K}$$

$$0\ \text{kg m}^{-3} \leq \rho \leq 650\ \text{kg m}^{-3} \qquad (11)$$

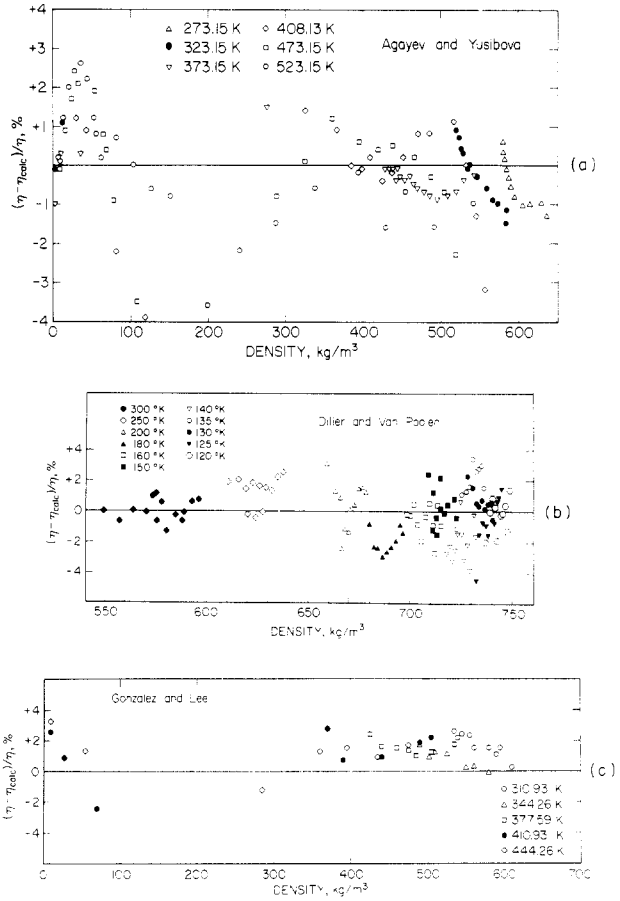

Figure 8. Comparison between the experimental data of Agayev and Yusibova (*7*), of Diller and Van Poolen (*8*), and of Gonzalez and Lee (*22*) and our representative equation for the viscosity.

Table IV. Values of the Parameters in Eq 7–10 for the Viscosity

$H_{00} = 0.0553$	$H_{20} = 5.901044$
$H_{01} = 0.0434$	$H_{21} = 0.542189$
	$H_{22} = 0.027622$
$H_{11} = 0$	$H_{23} = 0.270797$
$H_{12} = 11.230176$	$H_{24} = 0.063291$
$H_{13} = 0$	
$H_{14} = 0$	$z = T_c/10\ \text{K} = 40.784$
$H_{15} = 4.963725$	$\bar{T}_0 = 273.15\ \text{K}/T_c = 0.66975$
$H_{16} = -4.097720$	
$H_{17} = 0.995739$	

Table V. Viscosity Values Calculated from Eq 7 and Thermal Conductivity Values Calculated from Eq 12

	ρ, kg m^{-3}					
T, K	0	150	250	350	450	550
	Viscosity, μPa s					
300	7.504					148.203
410	10.182	18.561	28.225	44.492	77.540	150.882
500	12.208	20.587	30.251	46.518	79.565	152.907
600	14.303	22.682	32.346	48.613	81.661	155.003
	Thermal Conductivity, W m^{-1} K^{-1}					
300	0.0163					0.0884
410	0.0287	0.0512	0.0769	0.0714	0.0713	0.1009
500	0.0414	0.0520	0.0588	0.0673	0.0829	0.1135
600	0.0569	0.0666	0.0734	0.0826	0.0984	0.1290

It should be noted that experimental data for the viscosity in the vapor phase below 0 °C are not available, so that use of eq 7 in the vapor phase below 273.15 K involves an extrapolation with some possible loss of accuracy.

Table VI. Values of the Parameters in Eq 12–16 for the Thermal Conductivity

$L_{00} = 8.255070$	$L_{20} = 3.6218 \times 10^{-6}$
$L_{02} = 28.843455$	$L_{21} = 49.20$
$L_{05} = -1.896770$	$L_{22} = 0.28$
$L_{11} = 1.449797 \times 10^{-2}$	$y = (\gamma - \nu)/\gamma = 0.492$
$L_{14} = -0.320401 \times 10^{-3}$	
$L_{15} = 0.556972 \times 10^{-3}$	

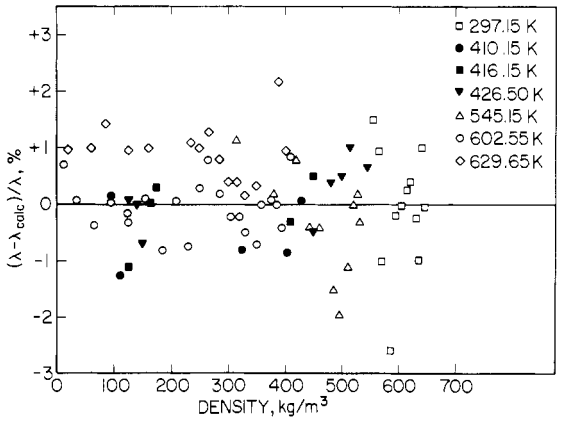

Figure 9. Comparison between the thermal conductivity data outside the critical region and our representative equation for the thermal conductivity.

In Table V we present viscosity values calculated from our representative equation (7) at selected temperatures and densities for computer program verification.

Representative Equation for Thermal Conductivity

Our proposed representative equation for the thermal conductivity of isobutane has the form

$$\bar{\lambda} = \bar{\lambda}_0(\bar{T}) + \bar{\lambda}_1(\bar{\rho}) + \bar{\lambda}_2(\bar{T},\bar{\rho}) \tag{12}$$

with

$$\bar{\lambda}_0(\bar{T}) = \frac{\bar{T}^{1/2}}{L_{00} + L_{02}/\bar{T}^2 + L_{05}/\bar{T}^5} \tag{13}$$

$$\bar{\lambda}_1(\bar{\rho}) = L_{11}\bar{\rho} + L_{14}\bar{\rho}^4 + L_{15}\bar{\rho}^5 \tag{14}$$

$$\bar{\lambda}_2(\bar{T},\bar{\rho}) = \frac{L_{20}}{\bar{\eta}}\left(\frac{\bar{T}}{\bar{\rho}}\right)^2\left(\frac{\partial\bar{P}}{\partial\bar{T}}\right)_\rho^2\left[\bar{\rho}\left(\frac{\partial\bar{\rho}}{\partial\bar{P}}\right)_T\right]^y F(\bar{T},\bar{\rho}) \tag{15}$$

and where

$$F(\bar{T},\bar{\rho}) = \bar{\rho}^{1/2}\exp[-L_{21}(\bar{T}-1)^2 - L_{22}(\bar{\rho}-1)^4] \tag{16}$$

The terms kept in eq 13 and 14 were determined from our experimental data, again with the aid of the optimization procedure of Wagner (*24–26*). The values of the coefficients L_{ij} and the exponent y are presented in Table VI.

The term $\bar{\lambda}_0(\bar{T})$ represents the thermal conductivity of the dilute gas as a function of temperature. The deviations of our experimental data as well as of the data of Kazaryan and Ryabstev (*9*) and of the value reported by Lambert et al. (*10*) from the values calculated with our equation are shown by Figure 1b. Our equation reproduces these experimental data to within about 2%.

The term $\bar{\lambda}_1(\bar{\rho})$ represents the excess thermal conductivity outside the critical region. A comparison of the equation and our experimental data outside the critical region is presented in Figure 9. The equation reproduces these data within about 2%.

The term $\bar{\lambda}_2(\bar{T},\bar{\rho})$ represents the additional enhancement of the thermal conductivity in the critical region. Equation 15 is

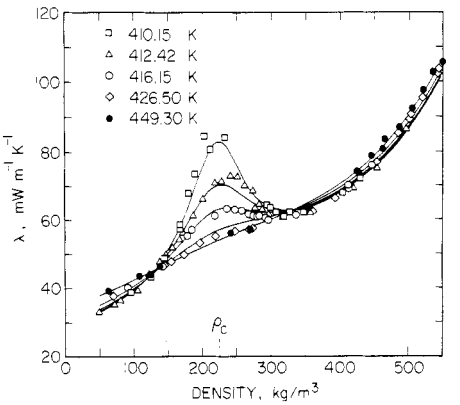

Figure 10. Thermal conductivity as a function of density at temperatures in the vicinity of the critical temperature. The solid curves represent the values calculated from eq 12.

the same as the equation used to represent the behavior of the thermal conductivity of steam in the critical region (*27*, *31*). In dimensional form eq 15 implies for the critical enhancement $\Delta\lambda = \lambda - \lambda_0 - \lambda_1$

$$\Delta\lambda = \frac{Rk_B T}{6\pi\eta\xi}\rho(c_p - c_v)F \tag{17}$$

where k_B is Boltzmann's constant, c_p the specific heat at constant pressure, c_v the specific heat at constant volume, ξ the correlation length, and R a constant (*27*, *31*, *32*). The correlation length ξ is calculated as (*32*, *33*)

$$\xi = \xi_0(\bar{\chi}_T/\Gamma)^{\nu/\gamma} \tag{18}$$

where $\nu = 0.63$ and $\gamma = 1.24$ are universal critical exponents for the correlation length ξ and the compressibility-like quantity $\bar{\chi}_T = \bar{\rho}(\partial\bar{\rho}/\partial\bar{P})_T$, and where $\xi_0 = 0.22$ nm and $\Gamma = 0.055$ are the corresponding critical amplitudes (*34*). For the coefficient R we find the value $R = 1.2$ which is larger than the predicted value $R = 1.0$, but similar to that found for the thermal conductivity of some other gases in the critical region (*30*).

A comparison between the representative eq 12 and the experimental thermal conductivity data at temperatures in the vicinity of the critical temperature is presented in Figure 10. The equation does account for the enhancement of the thermal conductivity in the critical region although there do exist some systematic differences. These differences are related to the lack of accuracy with which we are able to locate the densities where the thermal conductivity at supercritical temperatures reaches its maximum. At the critical temperature this thermal conductivity must diverge at the critical density ρ_c. The issue how the location of the maxima in the thermal conductivity isotherms varies with temperature is quite complicated (*35*, *36*), and its resolution will require further experimental and theoretical work. Because of its simplicity we have kept for practical use the same equation previously used to characterize the critical thermal conductivity enhancement $\Delta\lambda$ for carbon dioxide (*33*) and steam (*31*).

Outside the critical region eq 12 represents the thermal conductivity data for isobutane with an accuracy of about ±2% in a range of temperatures and densities approximately bounded by

$$290\ \text{K} \leq T \leq 630\ \text{K} \tag{19}$$

$$0\ \text{kg m}^{-3} \leq \rho < 650\ \text{kg m}^{-3}$$

In Table V we present thermal conductivity values calculated from eq 12 at selected temperatures and densities for computer program verification. The entries are chosen so that all contributions in eq 12 can be tested.

Acknowledgment

We acknowledge some stimulating discussions with R. D. Goodwin, B. Kamgar-Parsi and A. Nagashima.

Glossary

c_p	Specific heat at constant pressure
c_v	specific heat at constant volume
d	gap width between the two coaxial cylinders
$F(\bar{T},\bar{\rho})$	crossover function in eq 15
H_{ij}	coefficients in eq 8–10
K	cell constant in eq 4
k_B	Boltzmann's constant
L_{ij}	coefficients in eq 13–16
N_{Ra}	Rayleigh number
P	pressure
P_c	critical pressure
$\bar{P}$	reduced pressure ($=P/P_c$)
r	mean radius of annular fluid layer
R	amplitude in Stokes–Einstein diffusion law eq 17
Q	heat flow through fluid layer by conduction
Q_c	heat flow through fluid layer by convection
T	temperature
$\bar{T}_0$	parameter in eq 7
T_c	critical temperature
$\bar{T}$	reduced temperature ($=T/T_c$)
y	exponent in eq 15
z	parameter in eq 7
γ	exponent in eq 18
Γ	coefficient in eq 18
ΔT	temperature difference between cylinders
η	viscosity
η_0	viscosity in the limit $\rho \rightarrow 0$
η_1	excess viscosity ($=\eta(T,\rho) - \eta(T,0)$)
$\eta_r = 1$	reference viscosity (10^{-6} Pa s)
$\bar{\eta}$	dimensionless viscosity ($=\eta/\eta_r$)
ξ	correlation length
ξ_0	amplitude in eq 18
λ	thermal conductivity
λ_0	thermal conductivity in the limit $\rho \rightarrow 0$
λ_1	excess thermal conductivity ($=\lambda(T,\rho) - \lambda(T,0)$)
$\lambda_r = 1$	reference thermal conductivity (10^{-3} W m^{-1} K^{-1})
$\bar{\lambda}$	dimensionless thermal conductivity ($=\lambda/\lambda_r$)
$\Delta\lambda$	critical thermal conductivity enhancement
ν	exponent in eq 18
ρ	density
ρ_c	critical density
$\bar{\rho}$	reduced density ($=\rho/\rho_c$)
$\bar{\chi}_T$	symmetrized compressibility ($=\bar{\rho}(\partial\bar{\rho}/\partial\bar{P})_T$)

Registry No. Isobutane, 75-28-5.

Literature Cited

(1) Waxman, M.; Gallagher, J. S. *Proceedings of the 8th Symposium on Thermophysical Properties*; Sengers, J. V., Ed.; American Society of Mechanical Engineers: New York, 1982; Vol. I, p 88.
(2) Waxman, M.; Gallagher, J. S. *J. Chem. Eng. Data* **1983**, *28*, 224.
(3) Levelt Sengers, J. M. H.; Kamgar-Parsi, B.; Sengers, J. V. *J. Chem. Eng. Data* **1983**, *28*, 354.
(4) Diller, D. E.; Gallagher, J. S.; Kamgar-Parsi, B.; Morrison, G.; Rainwater, J. C.; Levelt Sengers, J. M. H.; Sengers, J. V.; Van Poolen, L. J.; Waxman, M. "Thermodynamic Properties of Isobutane-Isopentane Mixtures from 240 to 600 K and up to 200 MPa"; Internal Report 84-2971; National Bureau of Standards: Gaithersburg, MD, 1984.
(5) Goodwin, R. D.; Haynes, W. M. "Thermophysical Properties of Isobutane from 114 to 700 K at Pressures to 70 MPa"; NBS Technical Note 1051; U.S. Government Printing Office: Washington, DC, 1982.
(6) Kestin, J.; Khalifa, H. E.; Kumar, B. "Equilibrium and Transport Properties of Isobutane: A Survey of Available Data"; Report No. CAT-MEC/27/; Brown University: Providence, RI, 1978.
(7) Agayev, N. A.; Yusibova, A. D. *Gazov. Promst* **1969**, *14*(3), 41.
(8) Diller, D. E.; Van Poolen, L. J. *Int. J. Thermophys.* **1985**, *6*, 43.
(9) Kazaryan, V. A.; Ryabstev, N. I. *Gazov. Delo* **1969**, *10*, 27.
(10) Nieto de Castro, C. A.; Tufeu, R.; Le Neindre, B. *Int. J. Thermophys.* **1983**, *4*, 11.
(11) Ziebland, H. *Thermal Conductivity*; Tye, R. P., Ed.; Academic: New York, 1969; Vol. 2, p 65.
(12) Michels, A.; Sengers, J. V.; van de Klundert, L. J. M. *Physica (Amsterdam)* **1963**, *29*, 149.
(13) Sengers, J. V.; Bolk, W. T.; Stigter, C. J. *Physica (Amsterdam)* **1964**, *30*, 1018.
(14) Vidal, D.; Tufeu, R.; Garrabos, Y.; Le Neindre, B. *High Pressure Science and Technology*; Vodar, B., Marteau, H., Eds.; Pergamon: Oxford, 1980; p 692.
(15) Mann, W. B.; Dickens, B. G. *Proc. R. Soc. (London)* **1931**, *134A*, 77.
(16) Lambert, J. D.; Cotton, K. J.; Pailthorpe, M. W.; Robinson, A. M.; Scrivins, J.; Vale, W. R. F.; Young, R. M. *Proc. R. Soc. London* **1955**, *231A*, 280.
(17) Parkinson, C.; Gray, P. *J. Chem. Soc. Faraday Trans. 1* **1972**, *68*, 1065.
(18) Sengers, J. V. *Ber. Bunsenges. Phys. Chem.* **1972**, *76*, 234.
(19) Titani, T. *Bull. Chem. Soc. Jpn.* **1930**, *5*, 98.
(20) Sage, B. H.; Yale, W. D.; Lacey, W. N. *Ind. Eng. Chem.* **1939**, *31*, 223.
(21) Lipkin, M. R.; Davidson, J. A.; Kurtz, S. S. *Ind. Eng. Chem.* **1942**, *34*, 976.
(22) Gonzalez, M. H.; Lee, A. L. *J. Chem. Eng. Data* **1966**, *11*, 357.
(23) Abe, Y.; Kestin, J.; Khalifa, H. E.; Wakeham, W. A. *Physica A (Amsterdam)* **1979**, *97A*, 296.
(24) Wagner, W. *A New Correlation Method for Thermodynamic Data Applied to the Vapor-Pressure Curve of Argon, Nitrogen and Water*; IUPAC Thermodynamic Tables Project Centre: London, 1977.
(25) Ewers, J.; Wagner, W. *Proceedings of the 8th Symposium on Thermophysical Properties*; Sengers, J. V., Ed.; American Society of Mechanical Engineers: New York, 1982; Vol. I, p 78.
(26) de Reuck, K. M.; Armstrong, B. *Cryogenics* **1979**, *19*, 505.
(27) Kestin, J.; Sengers, J. V.; Kamgar-Parsi, B.; Levelt Sengers, J. M. H. *J. Phys. Chem. Ref. Data* **1984**, *13*, 175.
(28) Sengers, J. V.; Kamgar-Parsi, B. *J. Phys. Chem. Ref. Data* **1984**, *13*, 185.
(29) Basu, R. S.; Sengers, J. V. *Proceedings of the 8th Symposium on Thermophysical Properties*; Sengers, J. V., Ed.; American Society of Mechanical Engineers: New York, 1982; Vol. I, p 434.
(30) Sengers, J. V. *Int. J. Thermophys.* **1985**, *6*, 203.
(31) Sengers, J. V.; Watson, J. T. R.; Basu, R. S.; Kamgar-Parsi, B.; Hendricks, R. C. *J. Phys. Chem. Ref. Data* **1984**, *13*, 893.
(32) Basu, R. S.; Sengers, J. V. *Thermal Conductivity 16*; Larsen, D. C., Ed.; Plenum: New York, 1983; p 591.
(33) Sengers, J. V.; Levelt Sengers, J. M. H. *Progress in Liquid Physics*; Croxton, C. A., Ed.; Wiley: New York, 1978; p 103.
(34) Sengers, J. V.; van Leeuwen, J. M. J. *Int. J. Thermophys.* **1985**, *6*, 545.
(35) Sirota, A. M.; Latunin, V. I.; Belyaeva, G. M. *Therm. Eng.* (*Engl. Transl.*) **1976**, *23*(5), 59.
(36) Anisimov, M. A.; Kiselev, S. B.; Kostukova, I. G.; Rabinovich, V. A. *Proceedings of the 10th International Conference on the Properties of Steam*; Sytschev, V. V., Aleksandrov, A. A., Eds.; Mir: Moscow, 1986; Vol. I, p 435.

Received for review January 24, 1986. Accepted July 10, 1986. The work was performed as part of an international research program coordinated by the Subcommittee of IUPAC Commission I.2 on the transport properties of fluids. The research was supported by the Office of Standard Reference Data at the National Bureau of Standards and by the Pittsburgh Energy Technology Center of the Department of Energy under Grant No. DE-F622-85 PC 80505. Computer time for this project was provided by the Computer Science Center of the University of Maryland.